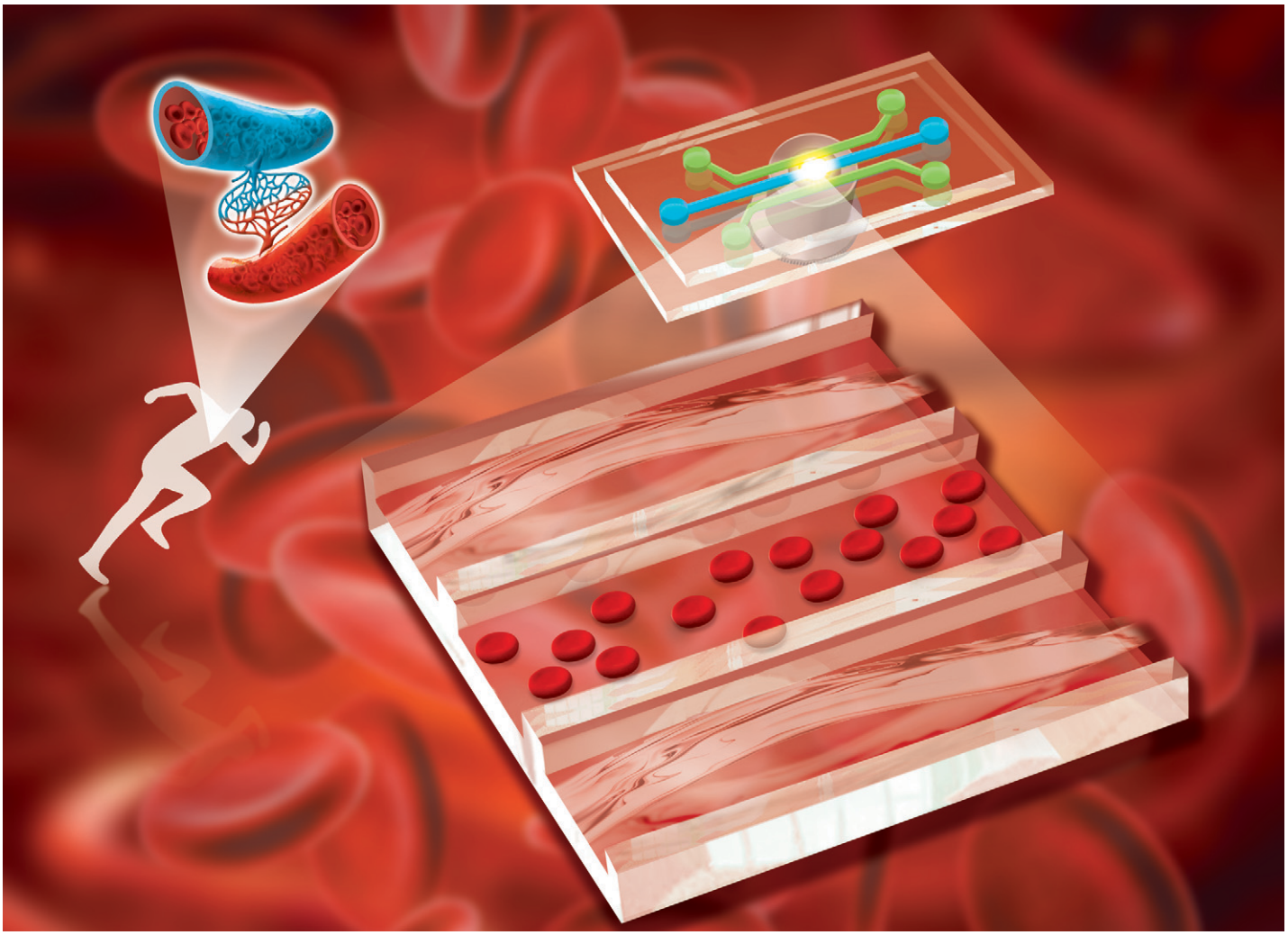

Featuring work from the Advanced Micro and Nanosystems Laboratory (AMNL) led by Prof. Yu Sun at the University of Toronto. The group develops micro and nano technologies for manipulating and characterizing cells, molecules, and nanomaterials.

Title: Mechanical differences of sickle cell trait (SCT) and normal red blood cells

A microsystem was developed for mechanical characterization of individual red blood cells (RBCs) under controlled oxygen conditions. RBCs from sickle cell trait individuals were found to be stiffer and more viscous than normal RBCs from healthy donors, and oxygen level variations did not alter their mechanical properties or morphology.

As featured in:

See Yi Zheng, Chen Wang, Yu Sun *et al.*, *Lab Chip*, 2015, **15**, 3138.

ROYAL SOCIETY OF CHEMISTRY

www.rsc.org/loc

Registered charity number: 207890

Lab on a Chip

PAPER

View Article Online
View Journal | View Issue

Cite this: *Lab Chip*, 2015, **15**, 3138

Mechanical differences of sickle cell trait (SCT) and normal red blood cells†

Yi Zheng,[ab] Mark A. Cachia,[a] Ji Ge,[a] Zhensong Xu,[a] Chen Wang*[de] and Yu Sun*[abc]

Received 13th May 2015,
Accepted 5th June 2015

DOI: 10.1039/c5lc00543d

www.rsc.org/loc

Sickle cell trait (SCT) is a condition in which an individual inherits one sickle hemoglobin gene (HbS) and one normal beta hemoglobin gene (HbA). It has been hypothesized that under extreme physical stress, the compromised mechanical properties of the red blood cells (RBCs) may be the underlying mechanism of clinical complications of sickle cell trait individuals. However, whether sickle cell trait (SCT) should be treated as physiologically normal remains controversial. In this work, the mechanical properties (*i.e.*, shear modulus and viscosity) of individual RBCs were quantified using a microsystem capable of precisely controlling the oxygen level of RBCs' microenvironment. Individual RBCs were deformed under shear stress. After the release of shear stress, the dynamic cell recovery process was captured and analyzed to extract the mechanical properties of single RBCs. The results demonstrate that RBCs from sickle cell trait individuals are inherently stiffer and more viscous than normal RBCs from healthy donors, but oxygen level variations do not alter their mechanical properties or morphology.

Introduction

Sickle cell disease (SCD) is a genetic disease caused by a mutation in the gene encoding the β-globin protein.[1] SCD patients possess abnormal hemoglobin (hemoglobin S, HbS) instead of normal hemoglobin (hemoglobin A, HbA). Under certain physiological conditions (*e.g.*, deoxygenation), the sickle hemoglobin (HbS) can polymerize into long chains, resulting in stiffened and often sickle-shaped red blood cells (RBCs). This triggers the obstruction of small vasculatures and causes clinical vaso-occlusive events.[1–4] The condition that a person inherits one sickle hemoglobin gene (HbS) and one normal beta hemoglobin gene (HbA) is described as sickle cell trait (SCT). Sickle cell trait individuals possess both HbS and HbA in their RBCs.[5–7] By the end of 2009, there were approximately 4 million people in the U.S. (1.31% of the population) and an estimated more than 300 million people worldwide with SCT.[5,8,9]

Given the prevalence of the SCT condition, relevant studies have been very limited compared to sickle cell disease since SCT had mostly been regarded as a benign condition and the cases that directly linked SCT to clinical complications are infrequent.[10,11] The debate over whether SCT should be treated as a benign condition is becoming more intensive over the past decade, especially after the National Collegiate Athletic Association (NCAA) initiated the practice of screening all Division I athletes for SCT in 2009.[11–13] Soon after, American Society of Hematology (ASH) along with several other organizations issued a policy statement contending that "current scientific evidence does not justify sickle cell trait screening as a prerequisite to athletic participation".[14]

The intense public disagreement necessitates both large-scale epidemiological studies and in-depth understanding of RBCs' physiology of SCT individuals.[8,9,15–18] Vaso-occlusion, the blockage of blood vessels caused by stiffened and often sickle-shaped RBCs usually occurs under deoxygenated conditions. It has been proven to be the most common and fatal symptom of sickle cells disease[19–21] and is also deemed to be the top contributor to sudden death of individuals with sickle cell trait.[17,18,22,23] Therefore, this study aims to reveal how the deformability of SCT RBCs differs from normal RBCs and whether they become stiffened and sickled under deoxygenation.

A number of technologies have been developed to characterize the mechanical properties of RBCs.[24,25] These technologies can be classified into two categories based on the testing environment is open or closed. Atomic force microscopy (AFM) and micropipette aspiration are two widely used open

[a] *Department of Mechanical and Industrial Engineering, University of Toronto, Toronto, ON, Canada. E-mail: sun@mie.utoronto.ca; Fax: +1 416 978 7753; Tel: +1 416 946 0549*
[b] *Institute of Biomaterials and Biomedical Engineering, University of Toronto, Toronto, ON, Canada*
[c] *Department of Electrical and Computer Engineering, University of Toronto, Toronto, ON, Canada*
[d] *Department of Pathology and Laboratory Medicine, Mount Sinai Hospital, Toronto, ON, Canada. E-mail: cwang@mtsinai.on.ca; Tel: +1 416 586 4469*
[e] *Department of Laboratory Medicine and Pathobiology, University of Toronto, Toronto, ON, Canada*

† Electronic supplementary information (ESI) available. See DOI: 10.1039/c5lc00543d

systems,[26,27] where RBCs are often tested in a droplet (or small volume) of medium that is exposed to the atmosphere. Because RBCs are sensitive to osmolality changes of the medium,[28,29] given the low measurement speed of these techniques (several minutes per cells), the small volume of medium can have significant osmolality changes during measurement. As a result, the measured mechanical properties of RBCs likely consist of artifacts caused by the variation of osmolality. For instance, an osmolality change of 300 mOsm to 200 mOsm can cause a 25–40% increase in the measured shear modulus value.[28,29] In addition, in order to control the oxygenation environment, a complicated system including a close chamber and medium exchange or gas exchange networks is required. This adds further complexity to the operation procedures, comprises measurement sensitivity, and leads to even lower measurement speeds.[30]

In closed systems, RBCs are tested in an enclosed environment (*e.g.*, microfluidic channels). A closed system can better maintain the osmolality of medium. Microfluidic measurement of RBCs also typically has a higher testing speed. In our previous work and others',[31–35] RBCs rapidly flows through microfluidic capillaries, and transit time and/or deformation index were used as indicators of RBCs' mechanical properties. However, these quantities, which are coupled with cell volume and adhesion properties, are not inherent material parameters of RBCs. Consequently, the values reported in the literature are usually not comparable. Leveraging the high gas permeability of PDMS, microfluidic devices capable of gas exchanges have been developed for controlling oxygen levels of cell culture.[36,37] Most recently, RBCs of sickle cell disease patients were investigated using such a microfluidic system, wherein flow resistance was used as a biophysical indicator of vaso-occlusive risk.[1,38]

Because of clinical and policy making interests, quantitatively investigating sickle cell trait RBCs' deformability and morphology under controlled oxygen conditions is the aim of this study. This study demands suitable tools capable of mechanically characterizing RBCs at the single cell level and varying the oxygen concentration while maintaining a physiological condition (*i.e.*, osmolality, pH, and hydration). Here we demonstrate a microsystem (Fig. 1(a)) for measuring the mechanical properties of individual RBCs under controlled oxygen levels. The device consists of three parallel microchannels separated by 100 μm thick PDMS membrane. A diluted blood sample is introduced to the central channel, and RBCs form adhesion to the device bottom. Two water tanks are connected to prevent the osmolality and pH changes caused by medium evaporation. The oxygen condition of tested RBCs is controlled by pumping either air or nitrogen into the two side channels. RBCs are deformed under shear stress generated using a regulated vacuum source. After the release of shear stress, the RBCs recover to their original shape. The dynamic recovery process is captured using microscopy imaging (Fig. 1(b)). Mechanical models are developed to extract the mechanical parameters (shear modulus and viscosity) of individual RBCs. Using this system, we measured the shear modulus and viscosity of SCT RBCs under oxygenated and deoxygenated conditions. Our results show that SCT RBCs are inherently stiffer and more viscous compared to normal RBCs from healthy donors, but oxygen level variations do not alter their mechanical properties and morphology.

Materials and methods

Blood specimens

Blood samples were collected from normal and sickle cell trait (SCT) individuals following the standard laboratory procedures in accordance with a research protocol approved by the Mount Sinai Hospital Review Board. Informed consent was obtained from all subjects. Blood samples were anticoagulated with ethylenediaminetetraacetic acid (EDTA, 1.5 mg ml^{-1}) and stored for no more than 48 hours. Before injected into the device, all blood samples were diluted 200 times in isotonic phosphate-buffered saline (PBS: 50 mM sodium phosphate, 90 mM NaCl, and 5 mM KCl, pH 7.4, 285 mosM).

Device fabrication and operation

The micro device was fabricated by bonding PDMS with grooves to a glass slide. The device consists of three parallel channels with a cross-sectional area of 40 μm × 300 μm. The channels are separated by 100 μm thick PDMS membrane, which facilitates gas exchange between the central channel and the two side channels. Before loading a diluted blood sample, the central channel was filled with PBS. After injecting the diluted blood sample to the central channel, the water tanks (also filled with PBS) were connected to the inlet and outlet carefully to avoid any bubbles present in the liquid pathway. RBCs were allowed to settle down for 20 minutes and form adhesion to the channel bottom due to negative surface charge. It should be noted that the purpose of using water tanks was to prevent the osmolality and pH changes caused by medium evaporation, instead of generating pressure differences. The capability of maintaining a constant osmolality for a long period is crucial for reliably measuring RBC properties since RBCs are highly sensitive to the ion concentration in medium. This microsystem is more advantageous compared to other popular tools for RBC mechanical properties (*e.g.*, micropipette aspiration and AFM), wherein RBCs are usually kept in an open droplet that can evaporate rapidly.

The water tanks are two closed containers with only one aperture connecting the space above the liquid surface to the atmosphere (atm.) or pressure control units (valve 1 and regulator). After loading the diluted blood sample and connecting the water tanks, measurement was conducted with the following protocol: (1) Flush the side channels with air by opening valve 3 for 10 min to achieve equilibrium of gas exchange. (2) Connect water tank 2 (T2) to atm. by opening valve 1 and closing the regulator. (3) Connect water tank

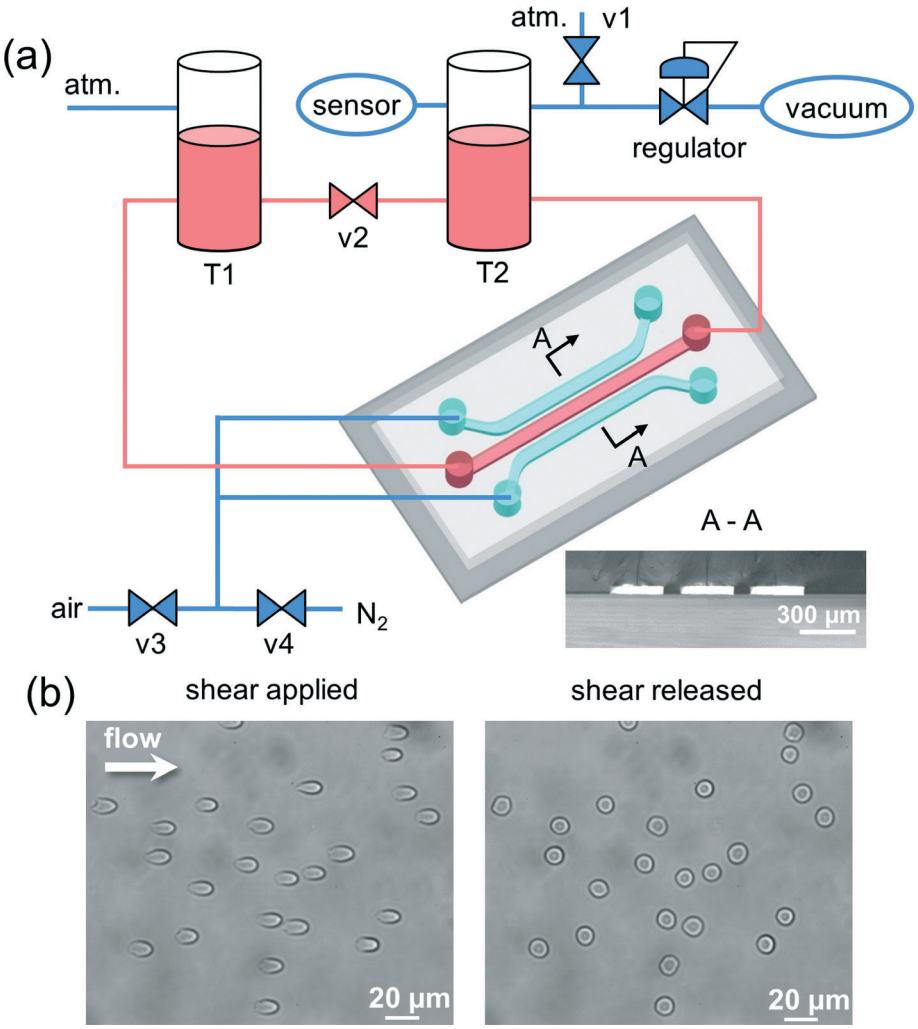

Fig. 1 Microsystem for studying mechanical properties (shear modulus and viscosity) of sickle cell trait (SCT) red blood cells (RBCs). (a) Device consists of three separated, parallel channels (see section A-A). Diluted blood samples are input into the central channel (red) connected to a water tank pressure control system. Gas exchange (air and N_2) in the two side channels (cyan) is controlled by valves 3 and 4. Valve 1 generates a step of pressure change to release shear stress in the central channel. (b) Left image shows deformed RBCs under shear stress. The RBCs adhered to the bottom of the central channel. After the release of shear stress, RBCs dynamically recover to their original shape. Right image is captured 1.5 seconds after the release of shear stress (see ESI† Video).

1 (T1) and water tank 2 (T2) by opening valve 2, and allow the water level to balance (10 min), thus the pressure difference within the central channels is zero. (4) Close valve 1 and valve 2, water tank 2 becomes a sealed container, connected only to the regulator. The regulator is used to adjust pressure difference for the application of shear stress. The pressure difference (−2 kPa in experiments) across the central channel was read from the pressure sensor connected to water tank 2. (5) After the application of the negative pressure (shear stress), RBCs are deformed. Valve 1 (solenoid valve) is then quickly opened to release pressure, and RBCs start to recover to their original shape. This complete dynamic process was recorded using a CCD camera (200 fps), through a 96× object on an inverted microscope. (6) For measuring the mechanical properties under deoxygenated condition, flush the side channels with N_2 by opening valve 4 and closing valve 3, repeat the above process. After the measurement under both oxygenation and deoxygenation was finished, a different field of view was imaged/measured.

Image processing

A custom-written MATLAB image processing program was used to measure cell length and width for quantifying the cell's deformation. Briefly, Otsu's adaptive thresholding method was used to binarize the image after Gaussian filtering. Cells located close to image edges and small contaminants were removed. Within each image, centroid and minimum bounding rectangle (MBR) of every cell were calculated and recorded. Cell length and width were determined from the MBR's dimensions. Since RBCs adhered to the microchannel bottom strongly, centroid displacement of a cell across the image sequence was smaller than 10 pixels. Therefore, cells with centroid displacement smaller than 10 pixels

across the sequential images were considered to be the same cell. Cell deformation was thus measured.

Oxygen diffusion validation

Prior to using the microsystem for RBC measurement, oxygen diffusion was validated by injecting an oxygen-sensitive luminescence probe (tris(4,7-diphenyl-1,10-phenanthroline)ruthenium(II) dichloride complex (1 mg ml^{-1} in PBS)) into the central channel (ESI† Fig. S1(a)). The luminescent intensity of this probe is quenched by oxygen molecules, and thus can reflect dissolved oxygen concentration of the solution. In experiments, luminescence was measured under illumination at 488 nm. Air (20% O_2 + 80% N_2) was flushed into the two side channels for 20 min, ensuring that equilibrium of the luminescent dye solution was reached. As shown in ESI† Fig. S1(b), gas was switched from air to N_2 at 0 s; after approximately 200 s, the luminescent intensity saturated, which indicates the completion of gas exchange.

Results and discussion

Mechanical models

In order to quantify the mechanical properties of RBCs, the Kelvin–Voigt model was applied to describe an RBC as a viscoelastic body. Shear modulus, which represents an RBC's resistance to shear stress-induced deformation, and viscosity, which describes an RBC's dynamic response to the rate of deformation, were determined using the following method.

The shear stress acting on RBCs on the central channel bottom can be estimated from the pressure difference ΔP (2 kPa used in experiments) and the channel geometry (assume $w \gg h$), according to

$$\tau = \frac{h}{2L} \times \Delta P \tag{1}$$

where L is the channel length and h is the channel height. Experimentally, the central channel's dimension is 40 μm (h) × 300 μm (w) × 6 cm (L).

To extract mechanical properties of RBCs from experimental data, Kelvin–Voigt model describes an RBC as a viscoelastic body.[39–42]

$$T = \frac{\mu}{2}\left(\lambda^2 - \frac{1}{\lambda^2}\right) + \eta \frac{2}{\lambda}\frac{\partial \lambda}{\partial t} \tag{2}$$

where T is the tension force acting on RBCs' membrane, μ is the shear modulus, η is the viscosity, λ is the extension ratio, and t is time.

At steady state before shear stress is released, μ can be calculated from T and λ.

$$\lambda = l/l_0 \tag{3}$$

where l is RBCs' length when deformed, and l_0 is RBCs' original length. The surface shape of deformed RBCs is approximated by an ellipse. T is estimated by balancing the force acting of the RBC surface.

$$T = \frac{\tau \times A}{l} \tag{4}$$

where τ is the shear stress acting on RBCs' surface, and A is the surface area of deformed RBCs. Hence, eqn (2) can be normalized by membrane shear modulus.

$$\frac{T}{2\mu} = \frac{1}{4}\left(\lambda^2 - \frac{1}{\lambda^2}\right) + t_c \frac{\partial \ln \lambda}{\partial t} \tag{5}$$

where $t_c \equiv \frac{n}{\mu}$ is the time constant that reflects cell dynamic response to force change. The time-dependent recovery of cell deformation is determined by

$$\lambda(t) = \left[\frac{\Lambda + e^{-t/t_c}}{\Lambda - e^{-t/t_c}}\right]^{\frac{1}{2}} \tag{6}$$

where $\Lambda \equiv \frac{\lambda_m^2 + 1}{\lambda_m^2 - 1}$, and t_c can be determined by fitting the dynamic process of shape recovery to eqn (6). Then viscosity is calculated with $\eta = \mu \times t$. Details of Kelvin–Voigt model were discussed elsewhere.[39–42] Note that using this model, although the cell shape effect can be compensated for, the slight variation of RBC shape and adhesion strength may still contribute to the measured mechanical properties.

Shear modulus and viscosity

After the release of shear stress (*i.e.*, connect water tank 2 to atmosphere by opening valve 1), deformed RBCs recover gradually to their original shape (see Fig. 2(a)). This dynamic process was captured *via* imaging at 200 Hz through an inverted microscope (96×, resolution: 0.23 μm $pixel^{-1}$). The extension ratio with respect to time was fitted to eqn (6). t_c that presents the best fitting result (*i.e.*, smallest R^2) was taken to be the time constant of the tested RBC. The shear modulus value (μ) was calculated using the steady state extension ratio (λ). Viscosity was obtained by the definition of $t_c \equiv \frac{\eta}{\mu}$. Fig. 2(a) shows a typical curve fitting result of a healthy RBC, and the microscopy images of the RBC's shape in corresponding image frames. The recovery process typically ends within 1.5 seconds (300 frames). Experimental data and curve fitting results are presented in blue and red, respectively ($R^2 > 0.99$ for all fitting results).

In the Kelvin–Voigt model, an RBC is modeled as a viscoelastic body and hence exhibits both viscous and elastic characteristics when undergoing deformation. Shear modulus and viscosity are used to depict these two properties, respectively, which ideally are supposed to be independent of each other. Fig. 2(b) is a scatter plot of the measured shear modulus and viscosity values of a control RBC sample (n = 71). No correlation was observed between the two parameters with

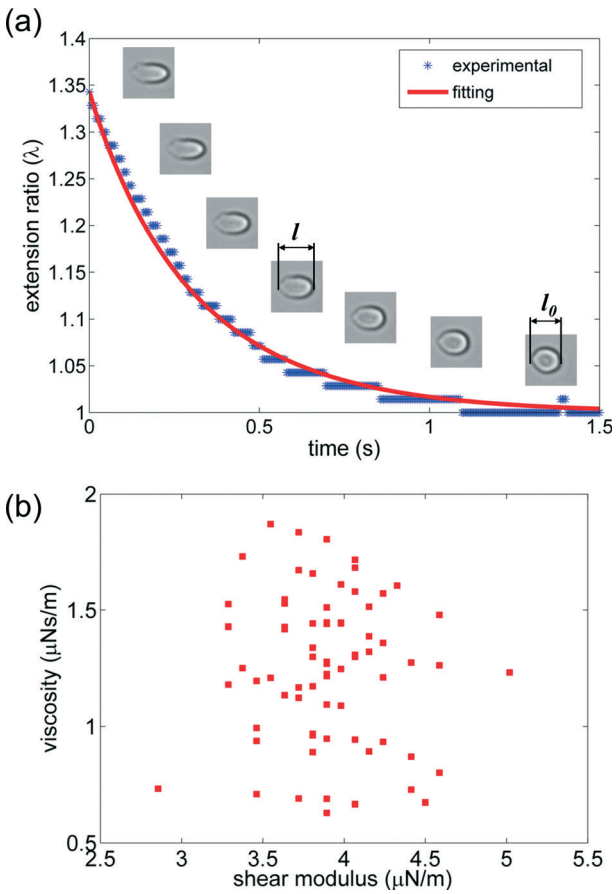

Fig. 2 (a) RBC dynamic shape recovery process. Shape recovery of an RBC fitted to the Kelvin–Voigt model. Microscopy images show RBC shape in corresponding image frames. Shear stress was released at 0 s. Recovery process typically ends within 1.5 seconds (300 frames). Experimental data and curve fitting results are presented in blue and red, respectively. (b) Scatter plot of shear modulus and viscosity of a control RBC sample (n = 71). No correlation was observed between the two parameters. Correlation coefficient R = 0.0612.

correlation coefficient of 0.0612. This corroborates that shear modulus and viscosity are two independent inherent material properties of RBCs.

Mechanical properties of SCT RBCs remain unchanged under different hypoxia conditions

Red blood cells from healthy donors (control) and sickle cell trait individuals were tested using the microsystem. Fig. 3(a) and (b) show the measured shear modulus and viscosity values of individual RBCs (n = 20) under oxygenated (blue) and deoxygenated (red) conditions. Fig. 3(a and b-bottom) summarize the percentage difference ($(\text{Value}_{de} - \text{Value}_{oxy})/\text{Value}_{oxy} \times 100\%$) of the two parameters obtained from the same cell (yellow for shear modulus and green for viscosity). The largest difference of the tested RBCs between oxygenated and deoxygenated conditions is approximately 6% with an average difference of 0.079% (shear modulus) and 0.43% (viscosity) for the healthy sample, and 0.96% and 0.33% for the SCT sample. Notably, the shear modulus and viscosity values under oxygenated and deoxygenated conditions (Fig. 3(a) and (b)) were measured on the same cells.

These results indicate that oxygen condition did not produce noticeable effect on mechanical properties for both healthy RBCs and SCT RBCs. Fig. 3(c) and (d) show the statistical presentation of the data in Fig. 3(a) and (b). Since there is virtually no difference of shear modulus and viscosity under different oxygen conditions, the median value of measured shear modulus and viscosity under oxygenated condition were used for comparison (shear modulus: 3.77 μN m^{-1} *vs.* 4.28 μN m^{-1}; viscosity: 1.13 μNs m^{-1} *vs.* 1.86 μNs m^{-1}). The mechanical property values of the healthy sample are in agreement with the values reported in the literature.[40,43,44] The SCT sample reveals both higher shear modulus and viscosity compared to healthy RBCs.

SCT RBCs are stiffer and more viscous than normal RBCs

In order to further verify this conclusion, shear modulus (see Fig. 4(a)) and viscosity (see Fig. 4(b)) from 5 control samples and 5 sickle cell trait samples were measured using the microsystem, where the three lines of the box represent 75 percentile, median, and 25 percentile; the whiskers represent the locations of maximum and minimum. For each sample, 60–80 RBCs were measured. As shown in Fig. 4(c), the shear modulus and viscosity differences of both healthy RBCs and SCT RBCs under oxygenation and deoxygenation are small (the average value of a blood sample is lower than 1%), demonstrating that healthy RBCs and sickle cell trait RBCs did not vary their mechanical properties in response to different oxygen conditions. The values measured under oxygenation were used as the inherent mechanical properties of the samples. Fig. 4(d) and (e) summarize average group median values of shear modulus and viscosity of healthy RBCs and SCT RBCs. Compared to healthy samples, SCT samples exhibit higher shear modulus (3.81 ± 0.24 μN m^{-1} *vs.* 4.42 ± 0.35 μN m^{-1}) and viscosity (1.22 ± 0.21 μNs m^{-1} *vs.* 1.75 ± 0.15 μNs m^{-1}), revealing that sickle cell trait RBCs are stiffer and more viscous. Mann–Whitney nonparametric analysis shows statistical difference exists between the healthy and SCT populations.

Sickle cell trait is an inherited protection mechanism of malaria endemic population and has a broad positive effect of child survival.[7–9] Although sickle cell trait was historically perceived as an asymptomatic condition, the concerns about exercise-related (or extreme physiological condition) morbidity and mortality have increased over the past decades.[8,9,11,45,46] Recent large-scale epidemiological data revealed connections between sickle cell trait and exercise-related mortality.[9] However, to date, it is still controversial that whether sickle cell trait is directly responsible for the unexplainable death. If the answer is yes, then what are the underlying pathophysiological mechanisms? Hemorheology studies suggest higher viscosity of the whole blood sample from sickle cell trait individuals under normal condition.[47–49] While some believe that sickle cell trait RBCs would

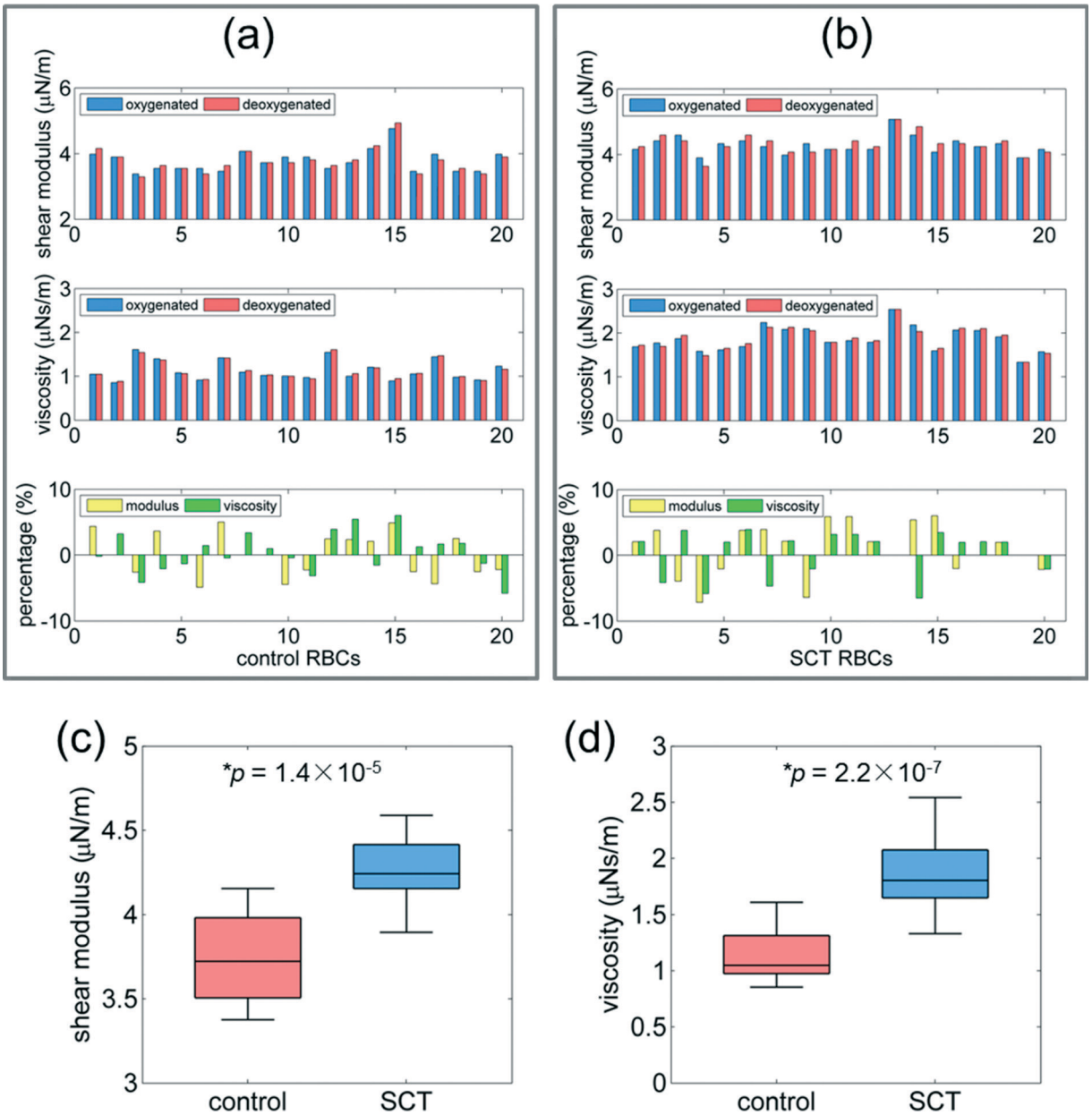

Fig. 3 Mechanical properties of control and SCT RBCs measured in one test (cell number n = 20). (a) and (b) Shear modulus (top) and viscosity (middle) of individual control and SCT RBCs under oxygenation (blue) and deoxygenation (red). Figures on the bottom summarize the percentage difference of the two parameters (yellow for shear modulus and green for viscosity) under the oxygenated and deoxygenated conditions ($(Value_{de} - Value_{oxy})/Value_{oxy} \times 100\%$). The largest difference is about 6 percent, with an average of 0.079% (shear modulus) and 0.43% (viscosity) for the control sample, and 0.96% and 0.33% for the SCT sample, elucidating that oxygen condition has no effect on altering mechanical properties of both control RBCs and SCT RBCs. (c) and (d) Statistical summary of the shear modulus and viscosity values in (a) and (b). Values measured under oxygenation are presented here. The RBCs from the SCT sample are stiffer and more viscous than the RBCs from the control sample. *p was calculated using Mann–Whitney nonparametric analysis.

polymerize and sickle, as sickle cell disease RBCs, the observed sickling of RBCs found in sudden-death of SCT individuals are likely caused by the artifacts of the death.[50,51] Existing results on mechanical properties of single RBCs from sickle cell trait individuals are limited.[26,52] The microsystem reported in this paper enabled quantification of the shear modulus and viscosity of single RBCs under controlled oxygen conditions. The experimental results demonstrate that RBCs from sickle cell trait individuals are inherently stiffer and more viscous compared to RBCs from healthy donors; however, oxygen level variations do not alter their mechanical properties and morphology.

The mechanical property differences of SCT RBCs, as compared to normal RBCs, can possibly be attributed to several physiological alterations. It was reported that SCT RBCs contain a higher concentration of Ca^{+2} involved in the regulation

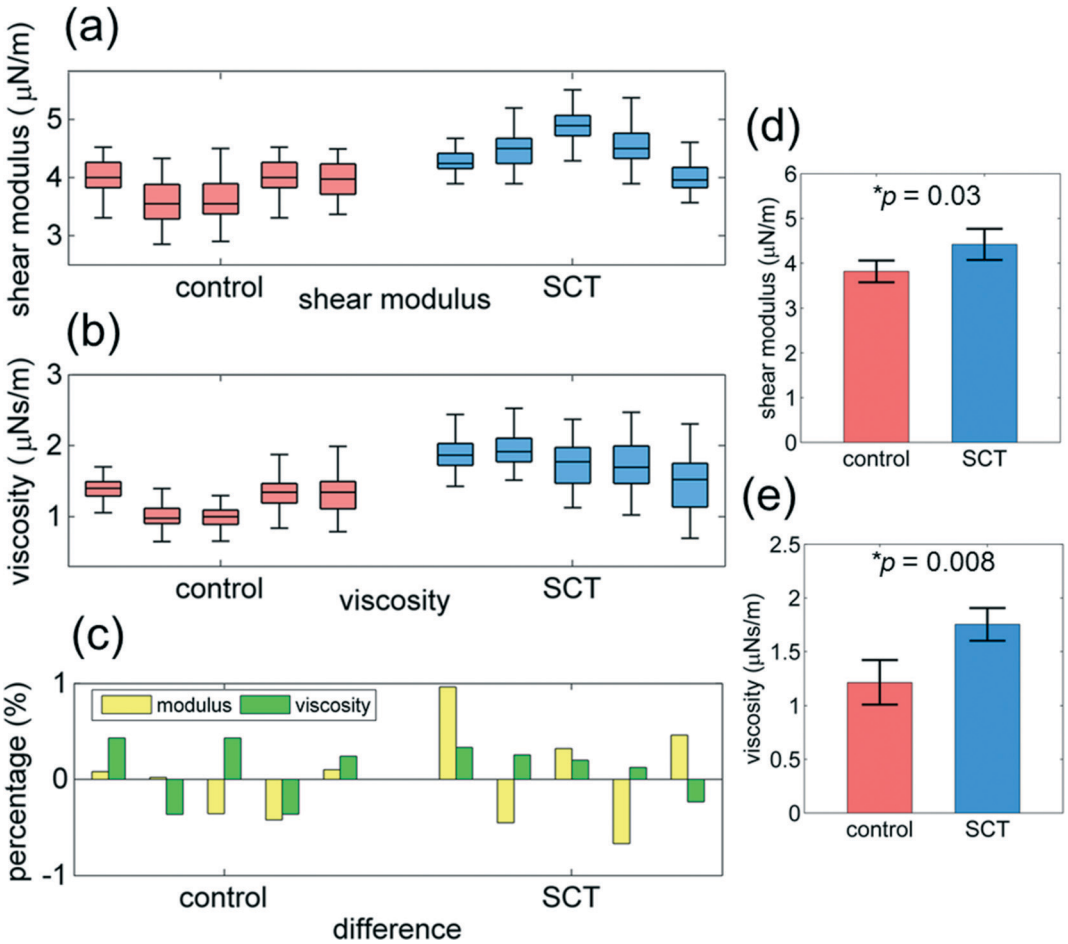

Fig. 4 Mechanical properties measured from 5 healthy/control samples (red) and 5 SCT samples (blue). For each sample, the three lines of the box represent 75 percentile, median, and 25 percentile; the whiskers represent the locations of maximum and minimum (n = 60–80 cells for each sample). (c) The percentage differences (average of individual RBCs) of tested samples under oxygenation and deoxygenation are within 1%. The average median values of shear modulus (d) and viscosity (e) of the 5 control samples and the 5 SCT samples are 3.81 ± 0.24 μN m^{-1} *vs.* 4.42 ± 0.35 μN m^{-1} and 1.22 ± 0.21 μNs m^{-1} *vs.* 1.75 ± 0.15 μNs m^{-1} (mean ± SE), respectively. *p was calculated using Mann–Whitney nonparametric analysis; and error bars represent standard error of the mean value. These results demonstrate that SCT RBCs are inherently stiffer and more viscous, as compared to control RBCs. In addition, their mechanical properties do not response to oxygen conditions.

of binding of band 3 to the cytoskeleton bound ankyrin. By enhancing the binding of spectrin, the increased Ca^{+2} can likely increase the rigidity of the RBC membrane.[26,53] Observed mechanical properties could also be due to the greater activity of the RBCs' K^{+}–Cl^{-} cotransporter and monocarboxylate transporter of SCT individuals, which can cause the disorganization of membrane integral proteins.[54,55] In addition, the higher viscosity of SCT RBCs is most likely related to the 20–40% hemoglobin S in the cytoplasm of SCT RBCs, since hemoglobin S is known to become more viscous when polymerized.[56]

Conclusion

Due to the growing public concerns such as athletic associations over the mortality and morbidity of young sickle cell trait athletes and the profound influence on millions of SCT people, interests in studying SCT RBCs have increased recently. Among many pathophysiological questions that remain to be answered, this work studied the mechanical properties (shear modulus and viscosity) of RBCs from SCT individuals. Our results demonstrate that RBCs from sickle cell trait individuals are significantly stiffer and more viscous than normal RBCs, but oxygen level variations do not alter their mechanical properties and morphology. Technically, the microsystem developed in this work enabled quantification of the mechanical properties of individual RBCs under controlled oxygen conditions. Next step is to involve a larger sample size to reveal the heterogeneity of the mechanical properties of SCT RBCs across SCT individuals and to comprehensively investigate their response to different oxygen conditions and other physiological factors such as pH changes.

Authorship contributions

Y. Z, Y. S. and C. W. designed the project. Y. Z. developed the mechanical models. Y. Z. and M. A. C. performed

experiments. Y. Z. and Z. X. processed data. J. G. developed the image processing algorithm. Y. Z, C. W and Y. S. discussed results and constructed the manuscript. All authors reviewed the manuscript.

Disclosure of conflicts of interest

The authors declare no competing financial interests.

Acknowledgements

Financial support from the Natural Sciences and Engineering Research Council of Canada (NSERC) through an E. W. R. Steacie Fellowship and from the Canada Research Chairs Program is acknowledged.

References

1 D. K. Wood, A. Soriano, L. Mahadevan, J. M. Higgins and S. N. Bhatia, *Sci. Transl. Med.*, 2012, **4**, 123ra26.
2 N. Lemonne, Y. Lamarre, M. Romana, M. Mukisi-Mukaza, M.-D. Hardy-Dessources, V. Tarer, D. Mougenel, X. Waltz, B. Tressières, M.-L. Lalanne-Mistrih, M. Etienne-Julan and P. Connes, *Blood*, 2013, **121**, 3054.
3 M. H. Steinberg, *N. Engl. J. Med.*, 1999, **340**, 1021.
4 L. H. Mackie and R. M. Hochmuth, *Blood*, 1990, **76**, 1256.
5 G. Tsaras, A. Owusu-Ansah, F. O. Boateng and Y. Amoateng-Adjepong, *Am. J. Med.*, 2009, **122**, 507.
6 J. Tripette, P. Connes, E. Beltan, T. Chalabi, L. Marlin, R. Chout, O. K. Baskurt, O. Hue and M.-D. Hardy-Dessources, *Clin. Hemorheol. Microcirc.*, 2010, **45**, 39.
7 P. A. Lang, R. S. Kasinathan, V. B. Brand, C. Duranton, C. Lang, S. Koka, E. Shumilina, D. S. Kempe, V. Tanneur, A. Akel, K. S. Lang, M. Föller, J. F. J. Kun, P. G. Kremsner, S. Wesselborg, S. Laufer, C. S. Clemen, C. Herr, A. A. Noegel, T. Wieder, E. Gulbins, F. Lang and S. M. Huber, *Cell. Physiol. Biochem.*, 2009, **24**, 415.
8 M. C. Caughey, L. R. Loehr, N. S. Key, V. K. Derebail, R. F. Gottesman, A. V. Kshirsagar, M. L. Grove and G. Heiss, Sickle Cell Trait and Incident Ischemic Stroke in the Atherosclerosis Risk in Communities Study, *Stroke*, 2014, 2863–2867.
9 L. B. Jordan, K. Smith-Whitley, M. J. Treadwell, J. Telfair, A. M. Grant and K. Ohene-Frempong, Screening U.S. college athletes for their sickle cell disease carrier status, *Am. J. Prev. Med.*, 2011, **41**, S406–S412.
10 P. Heller, W. R. Best, R. B. Nelson and J. Becktel, *N. Engl. J. Med.*, 1979, **300**, 1001.
11 N. S. Key and V. K. Derebail, *Hematology Am. Soc. Hematol. Educ. Program*, 2010, **2010**, 418.
12 B. A. Tarini, M. A. Brooks and D. G. Bundy, *BMC Health Serv. Res.*, 2012, **47**, 446.
13 K. G. Harmon, J. A. Drezner, D. Klossner and I. M. Asif, *Br. J. Sports Med.*, 2012, **46**, 325.
14 "Statement on screening for sickle cell trait and athletic participation," can be found under, http://www.hematology.org/Advocacy/Statements/2650.aspx, 2012.
15 J. A. Kark, D. M. Posey, H. R. Schumacher and C. J. Ruehle, *N. Engl. J. Med.*, 1987, **317**, 781.
16 B. L. Mitchell, *J. Natl. Med. Assoc.*, 2007, **99**, 300.
17 L. Scheinin and C. V. Wetli, *Am. J. Forensic Med. Pathol.*, 2009, **30**, 204–208.
18 D. P. Wirthwein, S. D. Spotswood, J. J. Barnard and J. A. Prahlow, *J. Forensic Sci.*, 2001, **46**, 399–401.
19 M. H. Steinberg, *N. Engl. J. Med.*, 1999, **340**, 1021.
20 W. A. Eaton and J. Hofrichter, *Adv. Protein Chem.*, 1990, **40**, 63.
21 C. T. Noguchi, D. A. Torchia and A. N. Schechter, *Proc. Natl. Acad. Sci. U. S. A.*, 1980, **77**, 5487.
22 M. L. Anzalone, V. S. Green, M. Buja, L. A. Sanchez, R. I. Harrykissoon and E. R. Eichner, *Med. Sci. Sports Exercise*, 2010, **42**, 3.
23 K. M. Harris, T. S. Haas, E. R. Eichner and B. J. Maron, Sickle Cell Trait Associated With Sudden Death in Competitive Athletes, *Am. J. Cardiol.*, 2012, **110**(8), 1185–1188.
24 D.-H. Kim, P. K. Wong, J. Park, A. Levchenko and Y. Sun, *Annu. Rev. Biomed. Eng.*, 2009, **11**, 203.
25 Y. Zheng, J. Nguyen, Y. Wei and Y. Sun, *Lab Chip*, 2013, **13**, 2464.
26 J. L. Maciaszek and G. Lykotrafitis, *J. Biomech.*, 2011, **44**, 657.
27 E. Shojaei-Baghini, Y. Zheng, M. A. S. Jewett, W. B. Geddie and Y. Sun, Mechanical characterization of benign and malignant urothelial cells from voided urine, *Appl. Phys. Lett.*, 2013, **102**, 123704.
28 J. Evans, W. Gratzer, N. Mohandas, K. Parker and J. Sleep, *Biophys. J.*, 2008, **94**, 4134.
29 Y. Park, C. A. Best, T. Kuriabova, M. L. Henle, M. S. Feld, A. J. Levine and G. Popescu, *Phys. Rev. E: Stat., Nonlinear, Soft Matter Phys*, 2011, **83**, 051925.
30 T. Itoh, S. Chien and S. Usami, *Blood*, 1992, **79**, 2141.
31 D. A. Fedosov, B. Caswell and G. E. Karniadakis, *Biophys. J.*, 2010, **98**, 2215.
32 A. M. Forsyth, J. Wan, P. D. Owrutsky, M. Abkarian and H. A. Stone, *Proc. Natl. Acad. Sci. U. S. A.*, 2011, **108**, 10986.
33 Y. Zheng, E. Shojaei-Baghini, A. Azad, C. Wang and Y. Sun, *Lab Chip*, 2012, **12**, 2560.
34 Y. Zheng, J. Chen, T. Cui, N. Shehata, C. Wang and Y. Sun, *Lab Chip*, 2014, **14**, 577.
35 H. Bow, I. V. Pivkin, M. Diez-Silva, S. J. Goldfless, M. Dao, J. C. Niles, S. Suresh and J. Han, *Lab Chip*, 2011, **11**, 1065.
36 J. F. Lo, E. Sinkala and D. T. Eddington, *Lab Chip*, 2010, **10**, 2394.
37 S. C. Oppegard, K.-H. Nam, J. R. Carr, S. C. Skaalure and D. T. Eddington, *PLoS One*, 2009, **4**, e6891.
38 J. M. Higgins, D. T. Eddington, S. N. Bhatia and L. Mahadevan, *Proc. Natl. Acad. Sci. U. S. A.*, 2007, **104**, 20496.
39 X. Liu, Z. Tang, Z. Zeng, X. Chen, W. Yao, Z. Yan, Y. Shi, H. Shan, D. Sun, D. He and Z. Wen, *Math. Biosci.*, 2007, **209**, 190.
40 S. Braunmüller, L. Schmid, E. Sackmann and T. Franke, *Soft Matter*, 2012, **8**, 11240.
41 E. A. Evans, *Biophys. J.*, 1973, **13**, 941.

42 R. M. Hochmuth, P. R. Worthy and E. A. Evans, *Biophys. J.*, 1979, **26**, 101.
43 J. Guck, S. Schinkinger, B. Lincoln, F. Wottawah, S. Ebert, M. Romeyke, D. Lenz, H. M. Erickson, R. Ananthakrishnan, D. Mitchell, J. Käs, S. Ulvick and C. Bilby, *Biophys. J.*, 2005, **88**, 3689.
44 G. Tomaiuolo, M. Barra, V. Preziosi, A. Cassinese, B. Rotoli and S. Guido, *Lab Chip*, 2011, **11**, 449.
45 M. Diaw, A. Samb, S. Diop, N. D. Sall, A. Ba, F. Cisse and P. Connes, Effects of hydration and water deprivation on blood viscosity during a soccer game in sickle cell trait carriers, *Br. J. Sports Med.*, 2012, 326–331.
46 C. Y. Hooper, S. Fraser-bell, A. Farinelli and J. R. Grigg, *Graefe's Arch. Clin. Exp. Ophthalmol.*, 2006, **34**, 377.
47 P. Connes, M.-D. Hardy-Dessources and O. Hue, *J. Appl. Physiol.*, 2007, **103**, 2138.
48 J. Tripette, M. D. Hardy-Dessources, F. Sara, M. Montout-Hedreville, C. Saint-Martin, O. Hue and P. Connes, Does repeated and heavy exercise impair blood rheology in carriers of sickle cell trait?, *Clin. J. Sport Med.*, 2007, **17**(6), 465–470.
49 P. Connes, O. Hue, J. Tripette and M. D. Hardy-Dessources, in *Clin. Hemorheol. Microcirc.*, 2008, pp. 179–184.
50 E. S. Roach, *Arch. Neurol.*, 2005, **62**, 1781.
51 M. F. Bergeron, J. G. Cannon, E. L. Hall and A. Kutlar, *Clin. J. Sport Med.*, 2004, **14**, 354.
52 M. M. Brandao, A. Fontes, M. L. Barjas-Castro, L. C. Barbosa, F. F. Costa, C. L. Cesar and S. T. O. Saad, *Eur. J. Haematol.*, 2003, **70**, 207.
53 F. Liu, H. Mizukami, S. Sarnaik and A. Ostafin, *J. Struct. Biol.*, 2005, **150**, 200.
54 O. Olivieri, D. Vitoux, F. Galacteros, D. Bachir, Y. Blouquit, Y. Beuzard and C. Brugnara, *Blood*, 1992, **79**, 793.
55 F. Sara, P. Connes, O. Hue, M. Montout-Hedreville, M. Etienne-Julan and M.-D. Hardy-Dessources, *J. Appl. Physiol.*, 2006, **100**, 427.
56 G. A. Barabino, M. O. Platt and D. K. Kaul, *Annu. Rev. Biomed. Eng.*, 2010, **12**, 345.

